



**HAL**  
open science

# Carboxypeptidase E Independently Changes Microtubule Glutamylation, Dendritic Branching, and Neuronal Migration

Chen Liang, Damien Carrel, Nisha K Singh, Liam L Hiester, Isabelle Fanget,  
Hyuck Kim, Bonnie L Firestein

► **To cite this version:**

Chen Liang, Damien Carrel, Nisha K Singh, Liam L Hiester, Isabelle Fanget, et al.. Carboxypeptidase E Independently Changes Microtubule Glutamylation, Dendritic Branching, and Neuronal Migration. *ASN neuro*, 2022, 14, pp.175909142110627. 10.1177/17590914211062765 . hal-04608764

**HAL Id: hal-04608764**

**<https://cnrs.hal.science/hal-04608764v1>**

Submitted on 11 Jun 2024

**HAL** is a multi-disciplinary open access archive for the deposit and dissemination of scientific research documents, whether they are published or not. The documents may come from teaching and research institutions in France or abroad, or from public or private research centers.


L'archive ouverte pluridisciplinaire **HAL**, est destinée au dépôt et à la diffusion de documents scientifiques de niveau recherche, publiés ou non, émanant des établissements d'enseignement et de recherche français ou étrangers, des laboratoires publics ou privés.



Distributed under a Creative Commons Attribution - NonCommercial 4.0 International License

# Carboxypeptidase E Independently Changes Microtubule Glutamylation, Dendritic Branching, and Neuronal Migration

Chen Liang<sup>1,2</sup>, Damien Carrel<sup>3,†</sup>, Nisha K. Singh<sup>1,2,†</sup>,  
Liam L. Hiester<sup>1</sup>, Isabelle Fanget<sup>3</sup>, Hyuck Kim<sup>1</sup>,  
and Bonnie L. Firestein<sup>1</sup> 

ASN Neuro  
Volume 14: 1–15  
© The Author(s) 2022  
Article reuse guidelines:  
sagepub.com/journals-permissions  
DOI: 10.1177/17590914211062765  
journals.sagepub.com/home/asn  


## Abstract

Neuronal migration and dendritogenesis are dependent on dynamic changes to the microtubule (MT) network. Among various factors that regulate MT dynamics and stability, post-translational modifications (PTMs) of MTs play a critical role in conferring specificity of regulatory protein binding to MTs. Thus, it is important to understand the regulation of PTMs during brain development as multiple developmental processes are dependent on MTs. In this study, we identified that carboxypeptidase E (CPE) changes tubulin polyglutamylation, a major PTM in the brain, and we examine the impact of CPE-mediated changes to polyglutamylation on cortical neuron migration and dendrite morphology. We show, for the first time, that overexpression of CPE increases the level of polyglutamylated  $\alpha$ -tubulin while knockdown decreases the level of polyglutamylation. We also demonstrate that CPE-mediated changes to polyglutamylation are dependent on the CPE zinc-binding motif and that this motif is necessary for CPE action on p150<sup>Glued</sup> localization. However, overexpression of a CPE mutant that does not increase MT glutamylation mimics the effects of overexpression of wild type CPE on dendrite branching. Furthermore, although overexpression of wild type CPE does not alter cortical neuron migration, overexpression of the mutant may act in a dominant-negative manner as it decreases the number of neurons that reach the cortical plate (CP), as we previously reported for CPE knockdown. Overall, our data suggest that CPE changes MT glutamylation and redistribution of p150<sup>Glued</sup> and that this function of CPE is independent of its role in shaping dendrite development but plays a partial role in regulating cortical neuron migration.

## Keywords

$\alpha$ -tubulin, carboxypeptidase E, p150<sup>Glued</sup>, polyglutamylation, zinc-binding motif

Received October 11 2019; Revised 1 November 2021; Accepted for publication 3 November 2021

## Introduction

Carboxypeptidase E (CPE; aka neurotrophic factor- $\alpha$ 1) is a member of the N/E subfamily of the M14 family of metallo-carboxypeptidases (Reznik & Fricker, 2001). It was discovered as a prohormone-processing enzyme in endocrine cells and neurons, where it is responsible for the proteolytic processing of peptide intermediates, generating bioactive hormones and neurotransmitters (Fricker & Snyder, 1982; Hook et al., 1982). CPE hydrolyzes single carboxyl-terminal amino acids from polypeptide chains with specificity for basic residues, that is., lysine or arginine, by coordinating with zinc ions. In addition to its enzymatic activity, CPE is involved in sorting and transporting hormone and neuropeptide intermediates, such as pro-insulin, pro-brain-derived neurotrophic

factor (BDNF), and pro-opiomelanocortin (Dhanvantari et al., 2003; Loh et al., 2002; Lou et al., 2005). In recent

<sup>1</sup>Department of Cell Biology and Neuroscience, Rutgers, The State University of New Jersey, Piscataway, NJ, USA

<sup>2</sup>Molecular Biosciences Graduate Program, Rutgers, The State University of New Jersey, Piscataway, NJ, USA

<sup>3</sup>SPPIN Laboratory, Université de Paris, Centre National de la Recherche Scientifique UMR 8003, Paris, France

<sup>†</sup>These authors contributed equally to this work.

### \*Corresponding Author:

Dr. Bonnie L. Firestein, Department of Cell Biology and Neuroscience, Rutgers, The State University of New Jersey, 604 Allison Road, Piscataway, NJ 08854-8082, USA  
Email: firestein@biology.rutgers.edu



years, studies have elucidated the importance of CPE in the nervous system. CPE<sup>-/-</sup> mice display a variety of neuronal deficits, including abnormal dendritic structure and spine morphology, neuronal degeneration, and deficits in learning and memory (Woronowicz et al., 2008; Woronowicz et al., 2010). A more recent study identified a new mutation in the *CPE* gene from a patient with Alzheimer's disease, suggesting the involvement of this mutation in Alzheimer's-related neurodegeneration, memory deficits, and depression (Cheng et al., 2016). Furthermore, CPE protects CA3 hippocampal neurons from stress-induced death and cognitive dysfunction (Xiao et al., 2021).

Microtubules (MTs) and microtubule-associated proteins (MAPs) play crucial roles in establishing proper neuronal morphology, intracellular transport, and migration in the cortex and hippocampus (Penazzi et al., 2016). To achieve diversity and complexity in function, MT dynamics must be precisely controlled. One of the most important mediators of such control is post-translational modification (PTM) of tubulins. Polyglutamylation represents a major PTM of tubulins in the brain (Audebert et al., 1994), and it is unique from other PTMs in that polyglutamyl chains exhibit variable lengths and are involved in regulating protein-binding affinity to MTs. Specifically, the MAPs, Tau, MAP1B, and MAP2, and kinesin motors, most efficiently bind to MTs that are modified with three glutamyl units, while the relative affinity of the binding of these proteins decreases with shorter or longer glutamyl chain lengths on MTs (Bonnet, 2001; Boucher et al., 1994; Larcher et al., 1996). More recently, it was reported that there is graded control of the binding of spastin to MTs, and spastin-mediated severing of MTs is regulated by polyglutamylation (Valenstein & Roll-Mecak, 2016). Specifically, modulation of spastin activity by polyglutamylation is biphasic and sensitive to glutamyl chain length.

Several polyglutamylases have been identified as members of the tubulin tyrosine ligase-like (TTL) protein family (Ikegami et al., 2006; Janke et al., 2005; van Dijk et al., 2007). Depending on the preference of the specific enzyme, glutamates can be added onto a Glu residue in the carboxyl terminus of either  $\alpha$ -tubulin or  $\beta$ -tubulin, initiating side chains or elongating existing chains to variable lengths (van Dijk et al., 2007). In contrast, deglutamylases regulate side chain length by removing glutamates from  $\alpha$ -tubulin or  $\beta$ -tubulin. Recent data suggest that members of the cytosolic carboxypeptidase (CCP) family act as deglutamylases (Kalinina et al., 2007; Rodríguez de la Vega et al., 2007). CCPs share a conserved zinc-binding motif, a consensus sequence within the M14 carboxypeptidase family that includes CPE (Gomis-Ruth et al., 1999). Similar to polyglutamylases, CCPs differ in their specificity for substrates and activity, either shortening long side chains or removing the branch point glutamates from  $\alpha$ -tubulin or  $\beta$ -tubulin (Rogowski et al., 2010). We recently found that CCPI overexpression supports neuroregeneration in a spinal cord model of neurotoxicity (Ramadan et al., 2021), pointing to a role for glutamylation in the maintenance of neuronal health and functionality.

In a previous study, we reported a role for CPE in the regulation of neuronal migration and dendrite morphology (Liang et al., 2019). We found that CPE carboxyl-terminal interaction with p150<sup>Glu<sup>ed</sup></sup>, a MT-binding protein, and anti-catastrophe factor, mediates effects on dendrite branching (Liang et al., 2019). Furthermore, CPE regulates the subcellular localization of p150<sup>Glu<sup>ed</sup></sup> (Liang et al., 2019). Since CPE shares a conserved zinc-binding motif with other reported deglutamylases, in the current study, we asked whether CPE plays a role in regulating tubulin polyglutamylation. Interestingly, by changing CPE levels, we found that in cells that overexpress CPE, tubulin polyglutamylation actually increases. Additionally, expression of CPE protein with a mutated zinc-binding motif, which has no effect on glutamylation, demonstrates that changes to glutamylation observed when CPE is overexpressed are necessary to promote CPE action on p150<sup>Glu<sup>ed</sup></sup> localization but are not responsible for CPE-mediated effects on neuronal migration and dendrite morphology.

## Methods

### DNA Constructs and RNA Interference

Full-length rat CPE protein was subcloned into pEGFP-C1 or pCAG. A mutant of CPE lacking amino acids required to bind zinc (CPE-H114A,E117A) was generated by site-directed mutagenesis of the pEGFP-C1-CPE full-length construct, with His114 mutated to Ala and Glu117 mutated to Ala. cDNA encoding the mutant form of CPE, CPE-H114A,E117A, was subcloned into pCAG-GFP. siRNA against CPE and the appropriate negative control were purchased from Life Technologies (CPE siRNA, Mouse S64324; CPE siRNA Rat S220210; negative control #1, cat# 4390743).

### Antibodies and Reagents

Mouse anti-CPE (BD 610758; RRID:AB\_398081) and mouse anti-microtubule-associated protein 2 (MAP2; BD 556320; RRID:AB\_396359) were from BD Pharmingen. The mouse monoclonal antibody against dynactin p150<sup>Glu<sup>ed</sup></sup> (SC-135890; RRID:AB\_2090598) was from Santa Cruz. Rabbit anti-pericentrin (ab4448; RRID:AB\_304461), rabbit anti-alpha-tubulin (ab18251; RRID:AB\_2210057), and rabbit anti-detyrosinated-tubulin (ab3201; RRID:AB\_177350) were from Abcam. Mouse anti-polyglutamylated-tubulin (B3) (T9822; RRID:AB\_477598) was from Sigma. Rabbit anti-acetyl-alpha-tubulin (5335 s; RRID:AB\_10544694) was from Cell Signaling. The antibody against green fluorescent protein (GFP; chicken; PA1-9533; RRID:AB\_1074893) was purchased from ThermoFisher.

The COS-7 (CRL-1651, RRID:CVCL\_0224) and Neuro2a (CCL-131, RRID:CVCL\_0470) cell lines are commercially available from American Type Culture Collection.

### COS-7 Cell Transfection and Immunocytochemistry

COS-7 cells (15,800 cells/cm<sup>2</sup>) were seeded on coverslips previously coated with 0.1 mg/ml poly-D-lysine. One day after plating, cells were transfected with pEGFP-C1, pEGFP-C1-CPE, or pEGFP-C1-CPE-H114A,E117A using Lipofectamine 2000 (ThermoFisher) following the manufacturer's protocol. Forty-eight hours after transfection, cells were fixed with 4% paraformaldehyde (PFA) in phosphate-buffered saline (PBS) for 15 min and immunostained with indicated antibodies, followed by Hoechst 33,225 dye nuclear staining. Using Fluoromount G (Southern Biotechnology; Birmingham, AL), coverslips were mounted onto glass slides for imaging.

### Immunofluorescent Microscopy and p150<sup>Glued</sup> Localization Analysis

Analysis was performed as we have previously reported (Liang et al., 2019). We used COS-7 cells for this assay to compare our results to those we have published (Liang et al., 2019) and due to the fact that it is easier for us to visualize the centrosome in COS-7 cells than in Neuro2a cells. COS-7 cells were imaged at 600x using an Olympus Optical (Tokyo, Japan) IX50 microscope and fluorescent imaging system. To determine p150<sup>Glued</sup> localization, a straight line was drawn across the cell through the pericentri-positive centrosome and nucleus. The percentage of p150<sup>Glued</sup> concentrated on the centrosome was determined by plotting the intensity of p150<sup>Glued</sup> and pericentrin along the line drawn. The intensity of p150<sup>Glued</sup> fluorescence was measured within the peak of pericentrin (value A), and p150<sup>Glued</sup> fluorescence within 1  $\mu$ m of the pericentrin peak was measured (value B). The percentage of p150<sup>Glued</sup> localized to the centrosome was defined as the ratio of A to B.

### Fractionation and Western Blot Analysis of Neuro2a Cell Lysates

Neuro2a cells were plated at 40%–50% confluence in 60 mm dishes and transfected 24 h after plating with pEGFP-C1, pEGFP-C1-CPE, or pEGFP-C1-CPE-H114A,E117A using Lipofectamine LTX Plus or transfected with negative control siRNA or CPE siRNA using Lipofectamine RNAiMax, following the manufacturer's protocols. Cells were collected 2 days after transfection into prewarmed (37°C) MT stabilization and cell lysis buffer (100 mM PIPES [pH 6.9], 5 mM EGTA, 5 mM MgCl<sub>2</sub>, 20% glycerol, 0.5% Nonidet P40, 0.5% Triton X-100, and protease inhibitor cocktail [Cytoskeleton, Inc., cat# PIC02]), modified from a previous study (Audebert et al., 1993). Cells were homogenized, and the extract was centrifuged at 350 x g at room temperature for 5 min to pellet unbroken cells and tissue debris. The supernatant was collected and centrifuged at 100,000 x g at 37°C for 1 h to fractionate soluble and cytoskeletal proteins.

Pelleted cytoskeletal proteins were depolymerized and denatured by incubation with 8 M urea for 1 h. Equal volumes of protein samples were resolved by SDS-PAGE, and resolved proteins were transferred to polyvinylidene fluoride (PVDF) membranes. Membranes were probed for polyglutamylated-tubulin, acetylated-tubulin, detyrosinated-tubulin, and alpha-tubulin. Immunoreactive bands were visualized with HyGlo Quick Spray (Denville Scientific; South Plainfield NJ), and resulting films were quantified with ImageJ software (NIH).

### Coimmunoprecipitation

Twenty-four hours after plating, Neuro2a cells were transfected with pEGFP-C1, pEGFP-C1-CPE, or pEGFP-C1-CPE-H114A, E117A using Lipofectamine LTX Plus. Forty-eight hours after transfection, cells were scraped into HEPES/sucrose buffer (20 mM HEPES [pH 7.5], 320 mM sucrose, 1 mM EDTA, 5 mM DTT, 1 mM PMSF) and homogenized. Extracts were centrifuged to pellet unbroken cells or tissue debris, supernatant was collected, and cytosolic proteins were fractionated by centrifugation. Cytosolic fractions were precleared with protein G agarose (50% slurry (GE Healthcare, Piscataway, NJ, USA)) for 1 h, and after the addition of 0.05% bovine serum albumin (BSA), proteins were immunoprecipitated with monoclonal dynactin p150<sup>Glued</sup> antibody at 4°C overnight. Protein G agarose was added, and the samples were incubated for 1 h. Immunoprecipitates were washed with 0.1% Triton X-100, 50 mM Tris, pH 7.4, 300 mM NaCl, 5 mM EDTA, 0.02% NaN<sub>3</sub>, proteins were eluted, and eluates were resolved by SDS-PAGE. Proteins were transferred to PVDF membranes, which were probed for the indicated proteins. HyGlo Quick Spray (Denville Scientific; South Plainfield, NJ, USA) was used to visualize immunoreactive bands, and films were quantified using ImageJ software (NIH).

### In Utero Electroporation, Histological Procedures, Microscopy, and Migration Analysis

*In utero* electroporation was performed as we previously reported (Liang et al., 2019; Carrel et al., 2015). Briefly, pregnant Swiss mice were anesthetized at gestation day 14.5 (E14.5) with isoflurane, and the uterine horns were exposed in the abdominal cavity. Pulled glass capillaries (Drummond Scientific, Broomall, PA, USA) were used to inject plasmids (1–3  $\mu$ l of 2–2.5  $\mu$ g/ $\mu$ l stock) through the uterus into the lateral ventricles of embryos. Embryos were co-injected with 1 mg/ml Fast Green (Sigma). The heads of the embryos were placed between tweezer-type electrodes and electroporated as we described in (Liang et al., 2019; Carrel et al., 2015). Embryos developed *in utero* for 3 days post-electroporation, and the brains were dissected and fixed in 4% PFA in PBS for 48 h at 4°C. Brains were cryoprotected

in 30% sucrose in PBS, frozen in PolyFreeze (Sigma), and sectioned coronally at 16  $\mu\text{m}$ . A Zeiss Axio Observer.Z1 microscope using a 20X numerical aperture (NA) 0.8 objective with a Clara E CCD Camera (Andor Technology Limited, Belfast, UK) was used to image the sections.

### *In Vivo* Neuronal Migration Analysis

TagRFP-positive cells were counted using ImageJ (<http://rsb.info.nih.gov/ij/>; National Institutes of Health, Bethesda, Maryland). Cortical regions of interest containing positive cells were manually selected using nuclei stained with Hoechst 33,225 as a guide. For local migration analyses, the CP was divided into three equivalent regions of interest. A combination of ImageJ built-in minimum and unsharp mask filters were used to enhance the signal of cell bodies and lower the signal in the processes. Cells were automatically counted as local maxima. The same level of noise tolerance for a given set of experiments was maintained (and after validation of this level by manual counting of three to four sections). To standardize, we used median sections in a series containing transfected cells (two sections per brain at E20, separated by at least 48  $\mu\text{m}$ ) and discarded brains that did not meet these two criteria. The number of transfected neurons counted was normalized to the total number of transfected neurons in the cortical region (for total cortical migration analyses) or in the CP. The experimenter was blinded to conditions during analysis.

### *In Vivo* Neuronal Morphology Analysis

TagRFP-positive cells were counted using ImageJ (<http://rsb.info.nih.gov/ij/>; National Institutes of Health, Bethesda, Maryland). For each section, the intermediate zone (IZ) was manually selected using nuclei stained with Hoechst 33,225 as a guide. Brightness and contrast of the image were adjusted as needed for optimal visualization of cells. A grid was overlaid on the image, and the number of unipolar, bipolar, and multipolar cells in each grid section within the IZ was counted. The number of multipolar neurons counted within the IZ was normalized to the total number of neurons counted in the IZ of a given section. The experimenter was blinded to conditions when analyzing images.

### Primary Neuronal Culture and Dendrite Branching Analysis

Primary cultures of hippocampal neurons were prepared as we described previously (Liang et al., 2019; Akum et al., 2004; Chen & Firestein, 2007). Tissue was mechanically dissociated, and cells were plated at a density of 10,500 cells/cm<sup>2</sup> on poly-D-lysine-coated coverslips and maintained in Neurobasal medium (ThermoFisher) supplemented with B27 (ThermoFisher), GlutaMAX (ThermoFisher), penicillin,

and streptomycin. Cultures were co-transfected with pCAG-mOrange and indicated CPE constructs using Lipofectamine LTX Plus (ThermoFisher) at day *in vitro* (DIV) 7, fixed at DIV 10, and immunostained for GFP and MAP2, a neuronal marker. An Olympus Optical (Tokyo, Japan) IX50 microscope and fluorescent imaging system was used to image the neurons, and dendrite morphology was assessed using our Bonfire analysis program (Kutzing et al., 2010; Langhammer et al., 2010). The experimenter was blinded to conditions when analyzing images.

### Statistical Analysis

All analyses were performed using GraphPad Prism (GraphPad Software; San Diego, CA, USA). Student's *t*-test or ANOVA followed by a multiple comparisons test was used when appropriate. All statistical tests used for each experiment are noted in the figure legends.

## Results

**CPE Protein Shares Homology with Reported Tubulin Deglutamylases.** Since CPE belongs to the M14 carboxypeptidase family, we performed multiple sequence alignment to identify conserved motifs among several members of the CCP family. Interestingly, CPE shows homology to cytosolic carboxypeptidase (CCP) 1, CCP4, CCP5, and CCP6, with highest homology at a majority of the putative active sites for substrate binding and catalysis (Figure 1) (Aloy et al., 2001). Carboxypeptidases demonstrate a preference for C-terminal basic amino acids, where they act to hydrolyze these C-terminal amino acids. CPE shares a zinc-binding motif with these carboxypeptidases, and this motif is conserved among M14 family members and is crucial for their enzymatic activity (Figure 1) (Gomis-Ruth et al., 1999). Moreover, our previous work demonstrated that CPE expression is evenly distributed throughout the dendrites of cortical neurons and co-localizes with  $\beta$ -III tubulin, further substantiating the possibility of a potential interaction between CPE and  $\beta$ -tubulin (Liang et al., 2019). Recent evidence suggests that several carboxypeptidases alter glutamylation levels of MTs (Rogowski et al., 2010), and thus, we asked whether CPE could change MT glutamylation in addition to its main protease activity (Hutton et al., 1987).

**Alterations in CPE Protein Levels Change Tubulin Polyglutamylation.** To investigate whether CPE changes PTM of MTs and specifically deglutamylation, we overexpressed or knocked down CPE protein in Neuro2a cells and examined changes to PTMs, including polyglutamylation, acetylation, and detyrosination, in both polymerized (cytoskeletal) MTs and free (soluble) tubulin pools. First, we confirmed CPE overexpression and CPE siRNA knockdown efficiencies in fractionated Neuro2a cell lysates (Figure 2A). We observed overexpression and efficient knockdown, respectively, in both cytoskeletal and soluble fractions

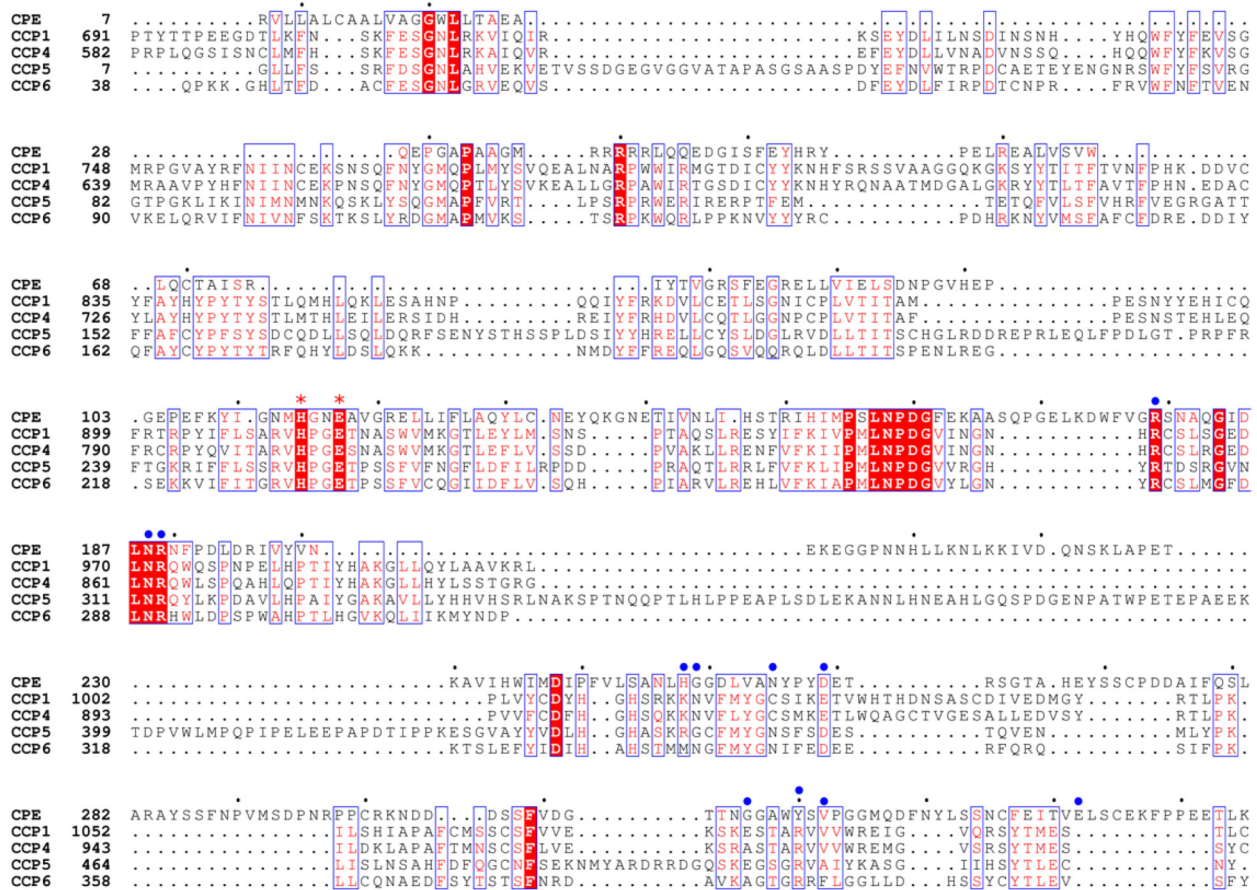


**Figure 1.** Carboxypeptidase E (CPE) protein shares homology with reported tubulin deglutamylases. Sequence alignment of mouse CPE protein and four reported tubulin deglutamylases: cytosolic carboxypeptidase (CCP) I, CCP4, CCP5, and CCP6. Sequences near the amino and carboxyl termini are not shown due to lack of homology with CPE. Conserved residues are shown in red boxes and white characters; conservatively changed residues are shown in red characters with blue frames. Red asterisks indicate the conserved zinc-binding motif, which was mutated to generate the CPE-H114A,E117A mutant construct used in this work. Blue dots indicate the putative active sites of CPE protein.

(Figure 2A). CPE was knocked down on average by 90% ( $n = 3$ ;  $p < 0.001$  as determined by paired Student's  $t$ -test). We then examined polyglutamylated levels of MTs and soluble tubulin pools. Surprisingly, in the cytoskeletal fractions of Neuro2a cells, we found that CPE overexpression resulted in increased levels of polyglutamylated  $\alpha$ -tubulin, while knockdown of CPE resulted in decreased polyglutamylated  $\alpha$ -tubulin (Figure 2B, C). This increase is modest,  $\sim 25\%$ , but it is significant. Polyglutamylated  $\alpha$ -tubulin levels remain the same in the soluble fractions of Neuro2a cells (Figure 2D, E). These results suggest that CPE plays a novel role, either directly or indirectly, in changing the polyglutamylated levels of tubulin. Furthermore, the effect of alterations in CPE levels is distinct from the functions previously reported for deglutamylases of the M14 carboxypeptidase family.

We next asked whether the effect of CPE on tubulin polyglutamylated levels is dependent on its zinc-binding motif, which is conserved among M14 carboxypeptidase family members (Gomis-Ruth et al., 1999). Although not much is known

about the role of zinc in regulating the deglutamylation activity of these proteins, it was previously reported that activity of the tubulin glutamylase, Nna1, increases in the presence of zinc (Wu et al., 2012). Thus, we generated a mutant form of CPE predicted to lack the capacity to bind zinc by substituting histidine 114 and glutamate 117, both in the zinc-binding motif, with alanines. Upon Western blot analysis of the cytoskeletal and soluble fractions of Neuro2a cell lysates, we observed that overexpression of this mutant, CPE-H114A, E117A, does not change the level of polyglutamylated  $\alpha$ -tubulin (Figure 2B–E). This result supports a role for CPE in influencing the polyglutamylated levels of tubulin and suggests that this activity of CPE is dependent on zinc binding.

To further investigate whether CPE changes additional PTMs of MTs, we analyzed the cytoskeletal and soluble Neuro2a lysate fractions for acetylated  $\alpha$ -tubulin and detyrosinated  $\alpha$ -tubulin. In contrast to that seen for polyglutamylated  $\alpha$ -tubulin, we observed no significant changes in either



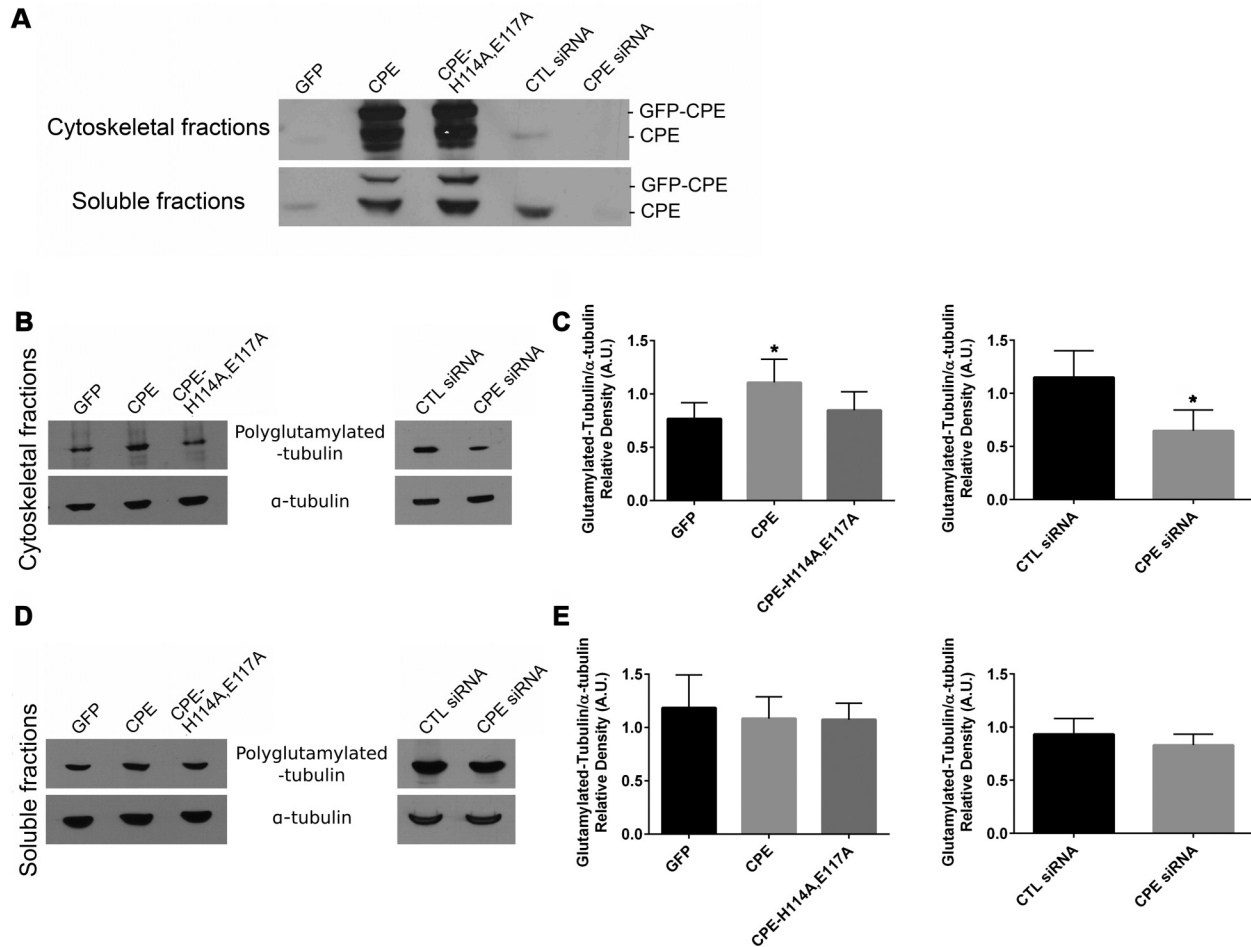


**Figure 2.** Alterations in carboxypeptidase E (CPE) protein levels result in changes to polyglutamylation of  $\alpha$ -tubulin. (A) Confirmation of overexpression of CPE and CPE-H114A,E117A and knockdown of CPE in Neuro2a cells. Neuro2a cells were transfected with pEGFP, pEGFP-CPE, pEGFP-CPE-CPE-H114A,E117A, control siRNA (CTL siRNA), or CPE siRNA. Cells were collected 48 h after transfection, and cytoskeletal and soluble proteins were fractionated and resolved by SDS-PAGE, transferred to polyvinylidene fluoride (PVDF) membranes, and membranes were immunoblotted for CPE. Representative blots are shown. (B) Western Blot analysis of polyglutamylation of tubulin in cytoskeletal fractions of Neuro2a cells. Cells were transfected with pEGFP, pEGFP-CPE, pEGFP-CPE-H114A,E117A, CTL siRNA, or CPE siRNA. Cells were collected and lysed 48 h after transfection. Cytoskeletal and soluble proteins were fractionated and resolved by SDS-PAGE, transferred to PVDF membranes, and membranes were immunoblotted for polyglutamylated  $\alpha$ -tubulin and total  $\alpha$ -tubulin. Left, representative blots of CPE overexpression and control conditions. Right, representative blots of CPE knockdown and control conditions. (C) Quantitation of polyglutamylated  $\alpha$ -tubulin levels normalized to total  $\alpha$ -tubulin levels and compared to control in cytoskeletal fractions. (D) Western Blot analysis of polyglutamylation of tubulin in soluble fractions of Neuro2a cells. Left, representative blots of CPE overexpression and control conditions. Right, representative blots of CPE knockdown and control conditions. (E) Quantitation of polyglutamylated  $\alpha$ -tubulin levels normalized to total  $\alpha$ -tubulin levels and compared to control in soluble fractions. Error bars indicate  $\pm$  SEM  $n = 6$  for all cytoskeletal fractions,  $n = 3$  for all soluble fractions. Outliers were excluded by Grubbs' test. \* $p < 0.05$  was determined by repeated measures one-way ANOVA followed by Tukey's multiple comparisons test (left panels) or paired Student's  $t$ -test (right panels). Note: AU = arbitrary units.

acetylation or detyrosination of tubulin as a result of alterations in CPE protein levels (Figure 3), suggesting that CPE specifically influences glutamylation.

**Overexpression of CPE Alters p150<sup>Glued</sup> Localization at the Centrosome and is Partially Dependent on the Zinc-Binding Motif.** We previously reported that CPE regulates the localization of its interactor, p150<sup>Glued</sup>, at the centrosome (Liang et al., 2019). Thus, we asked whether the CPE

zinc-binding motif and changes to tubulin polyglutamylation are involved in the regulation of p150<sup>Glued</sup> localization. To confirm that the mutated CPE protein, CPE-H114A,E117A, does indeed bind to p150<sup>Glued</sup>, we performed a co-immunoprecipitation assay. We expressed GFP, GFP-tagged CPE, or GFP-tagged CPE-H114A,E117A in Neuro2a cells and immunoprecipitated p150<sup>Glued</sup> from the cytosolic protein extract. We found that CPE-H114A,

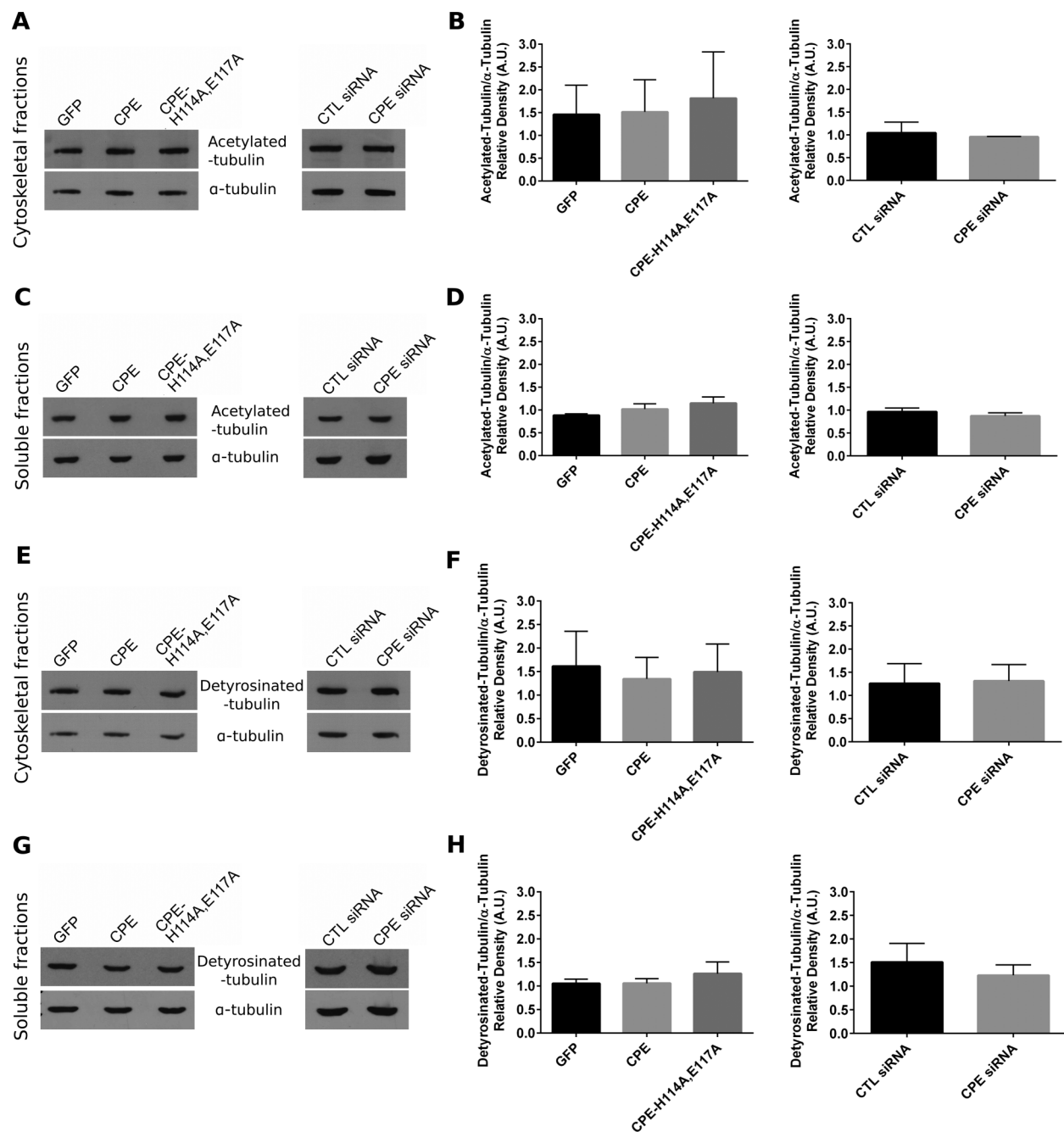


**Figure 3.** Alterations in carboxypeptidase E (CPE) protein levels do not affect levels of acetylated or detyrosinated  $\alpha$ -tubulin. (A) Western blot analysis of acetylated  $\alpha$ -tubulin in cytoskeletal fractions of Neuro2a cells. Cells were transfected with pEGFP, pEGFP-CPE, pEGFP-CPE-H114A,E117A, control (CTL) siRNA, or CPE siRNA. Cytoskeletal proteins were fractionated and resolved by SDS-PAGE, transferred to polyvinylidene fluoride (PVDF) membranes, and membranes were immunoblotted for acetylated  $\alpha$ -tubulin and total  $\alpha$ -tubulin. Representative blots are shown. (B) Quantitation of acetylated  $\alpha$ -tubulin levels/total  $\alpha$ -tubulin levels relative to control in cytoskeletal fractions. (C) Western blot analysis of  $\alpha$ -tubulin acetylation in soluble fractions of Neuro2a cells. Representative blots are shown. (D) Quantitation of acetylated  $\alpha$ -tubulin levels/total  $\alpha$ -tubulin levels relative to control in soluble fractions. (E) Western blot analysis of detyrosinated  $\alpha$ -tubulin in cytoskeletal fractions of Neuro2a cells. Cells were transfected with pEGFP, pEGFP-CPE, pEGFP-CPE-H114A, E117A, CTL siRNA, or CPE siRNA. Representative blots are shown. (F) Quantitation of detyrosinated  $\alpha$ -tubulin levels/total  $\alpha$ -tubulin levels relative to control in cytoskeletal fractions. (G) Western blot analysis of detyrosinated  $\alpha$ -tubulin in soluble fractions of Neuro2a cells. Representative blots are shown. (H) Quantitation of detyrosinated  $\alpha$ -tubulin levels/total  $\alpha$ -tubulin levels relative to control in soluble fractions. Error bars indicate  $\pm$  SEM,  $n = 3$  for all conditions. Note: AU = arbitrary units.



E117A co-immunoprecipitates with p150<sup>Glued</sup> at similar levels as wild type CPE (Figure 4A, B). We then transfected COS-7 cells with constructs encoding GFP, CPE, or CPE-H114A,E117A and analyzed the percentage of p150<sup>Glued</sup> protein localized at the centrosome using pericentrin as a marker. As we demonstrated previously (Liang et al., 2019), overexpression of CPE decreases p150<sup>Glued</sup> localization at the centrosome (Figure 4C, D). Interestingly, overexpression of the zinc-binding domain mutant CPE (CPE-H114A,E117A) partially attenuates the effect of CPE overexpression on p150<sup>Glued</sup> distribution (Figure 4C, D), as the percentage of p150<sup>Glued</sup> localized at the centrosome when CPE-H114A,E117A is overexpressed does not significantly differ from that observed with either GFP or CPE overexpression. Our results suggest partial involvement of the zinc-binding motif and tubulin polyglutamylation in the regulation of p150<sup>Glued</sup> localization by CPE. Our data also indicate that although the zinc-binding motif is necessary, it is not sufficient to promote CPE action on p150<sup>Glued</sup> localization.

**Overexpression of CPE-H114A,E117A Alters Cortical Neuron Migration.** As we demonstrated previously (Liang et al., 2019), CPE expression is required for proper cortical neuron migration. To investigate whether the zinc-binding motif of CPE and tubulin polyglutamylation regulate neuronal migration, we co-electroporated pTagRFP with GFP (control), GFP-tagged CPE, or GFP-tagged CPE-H114A, E117A constructs *in utero* into embryonic day (E)14.5 mouse brains and analyzed brain sections at E17.5. We assessed neuronal migration to the ventricular zone (VZ), intermediate zone (IZ), and cortical plate (CP). We observed a decrease in the percentage of neurons reaching the CP when CPE-H114A,E117A is overexpressed, although migration to different regions within the CP is unaffected (Figure 5A–C). Furthermore, overexpression of either wild type or mutant CPE results in a greater percentage of cells that demonstrate multipolar morphology in the IZ, suggesting that these cells have stopped migrating (Figure 5D–E). In contrast, overexpression of CPE does not alter overall cortical neuron migration or migration within the CP (Figure 5A–C). Migration and changes to morphology are regulated by independent mechanisms (reviewed in Tabata & Nagata, 2016). Although these results are surprising, they suggest that CPE regulates the two processes independently. These results suggest that the zinc-binding motif of CPE plays a role in cortical neuron migration. It may act in a dominant-negative manner by either inhibiting normal glutamylation induced by CPE or attenuating other processes that regulate neuronal migration.

**Overexpression of CPE-H114A,E117A Alters Dendritic Arborization in Cultured Hippocampal Neurons.** Based on our previous findings (Liang et al., 2019), we proposed that a balance of CPE protein levels may be required to maintain proper dendritic arborization in hippocampal neurons. We demonstrated that overexpression of CPE results in decreased dendrite branching proximal to the soma and that this effect is

dependent on its carboxyl terminus (Liang et al., 2019). To investigate whether CPE-mediated effects on dendritic arborization are dependent on CPE-mediated changes to tubulin polyglutamylation, we overexpressed CPE or CPE-H114A, E117A in rat hippocampal neuronal cultures at DIV 7 and examined dendrite morphology at DIV 10, a time when active branching occurs in our cultures (Banker & Goslin, 1988; Charych et al., 2006; Dotti et al., 1988). Sholl analysis demonstrates that overexpression of either CPE or CPE-H114A,E117A results in decreased dendrite branching proximal to the soma (0–12  $\mu$ m and 0–18  $\mu$ m, respectively; Figure 6A–C), suggesting that the regulation of proximal dendrite number by CPE is independent of the CPE zinc-binding motif, and most likely, CPE-mediated tubulin polyglutamylation.

## Discussion

Here, we identify a novel role for CPE in changes to polyglutamylation of MTs. We find that histidine 114 and glutamate 117, predicted to be involved in zinc-binding, are essential for this effect of CPE overexpression. We show that zinc-binding, which correlates with CPE-mediated changes to polyglutamylation, plays a role in redistribution of p150<sup>Glued</sup> from the centrosome; however, overexpression of a zinc-binding CPE mutant results in only a partial effect on p150<sup>Glued</sup> localization, suggesting additional CPE-mediated mechanisms. Overexpression of either CPE or CPE-H114A,E117A results in similar decreases to proximal dendrites in cultured neurons, but only overexpression of CPE-H114A,E117A alters cortical neuron migration. Taken together, our results suggest a novel role for CPE-mediated changes to polyglutamylation in MT motor localization independent of CPE effects on dendrite branching and neuron migration.

### Novel Function for CPE in Regulating Tubulin Polyglutamylation

Various patterns of polyglutamylation can be generated on MTs and confer specificity of MAPs and motor protein binding to MTs (Bonnet, 2001; Boucher et al., 1994; Larcher et al., 1996; Valenstein & Roll-Mecak, 2016). Therefore, it is of importance to understand how polyglutamylation is regulated. Since CPE shares a conserved zinc-binding motif with currently known deglutamylases of the CCP family (Rodriguez de la Vega et al., 2007; Gomis-Ruth et al., 1999; Rogowski et al., 2010), we explored the role of CPE in altering tubulin polyglutamylation. Surprisingly, we found that overexpression of CPE increases polyglutamylated  $\alpha$ -tubulin, while knockdown of CPE decreases polyglutamylation. In addition, CPE-mediated effects on polyglutamylation levels are dependent on its zinc-binding motif. These results indicate

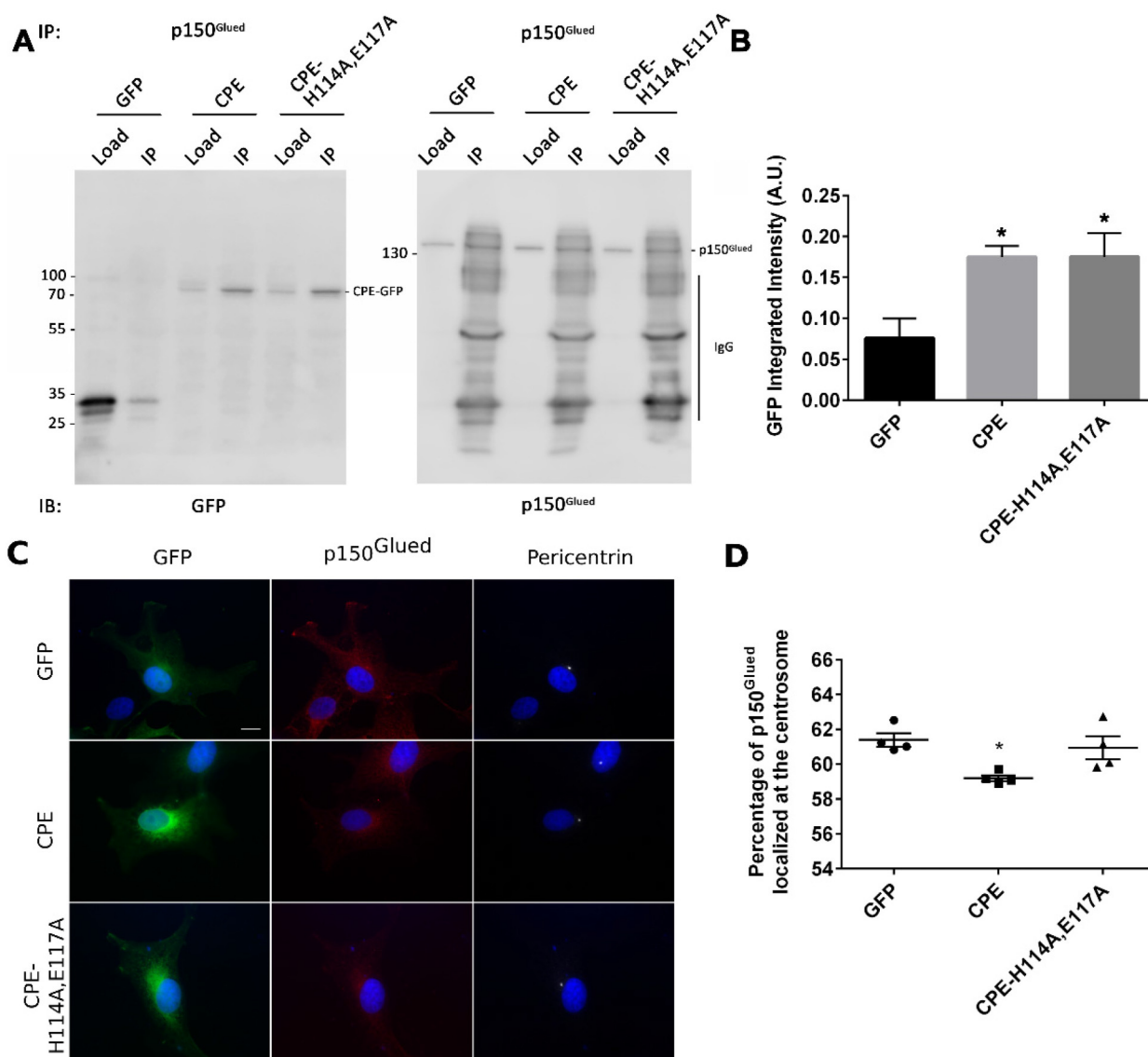


**Figure 4.** Overexpression of carboxypeptidase E (CPE) alters p150<sup>Glued</sup> localization at the centrosome and is partially dependent on the zinc-binding motif. (A) CPE and CPE-H114A,E117A co-immunoprecipitate with p150<sup>Glued</sup>. Neuro2a cells were transfected with GFP or CPE constructs. Cells were collected after 48 h, and proteins were extracted and subjected to immunoprecipitation with p150<sup>Glued</sup> antibody. Loading control (Load) and immunoprecipitates (IP) were resolved by SDS-PAGE. Proteins were transferred to PVDF membranes, and membranes were immunoblotted for GFP and p150<sup>Glued</sup>. Load represents 4% of extracted proteins. Uncropped, representative blots are shown. IgG bands (marked by the line) are present in the blot, confirming that p150<sup>Glued</sup> was immunoprecipitated with the p150<sup>Glued</sup> antibody since the same antibody was used for probing the blot and the IP. (B) Quantitation of GFP band intensities. Integrated density is the cumulative sum of pixel values (intensities) in the band that is detected for the GFP protein as measured using NIH ImageJ software. Error bars indicate  $\pm$  SEM, n = 5 for all conditions. \*p < 0.05 was determined by one-way ANOVA followed by Dunnett's multiple comparisons test. (C) Representative images showing p150<sup>Glued</sup> localization at the centrosome in COS-7 cells. COS-7 cells were transfected with GFP or CPE constructs. Cells were fixed at 48 h after transfection and immunostained with anti-GFP (green), anti-p150<sup>Glued</sup> (red), and anti-pericentrin (white), and nuclei were labeled with Hoechst dye (blue). Scale bar = 10  $\mu$ m. (D) Quantitation of the percentage of p150<sup>Glued</sup> proteins localized at the centrosome. For each independent experiment, 15–25 transfected cells of each condition were analyzed as described in Materials and Methods. Error bars indicate  $\pm$  SEM, n = 4 for all conditions. \*p < 0.05 was determined by repeated measures one-way ANOVA followed by Tukey's multiple comparisons test. Note: AU = arbitrary units.

a novel function for CPE in regulating tubulin polyglutamylation, either directly by acting on MTs or indirectly by altering other enzymes or signaling pathways.

The molecular mechanism underlying CPE action remains unclear, but one possible explanation is that CPE may form a complex with polyglutamylases or deglutamylases and

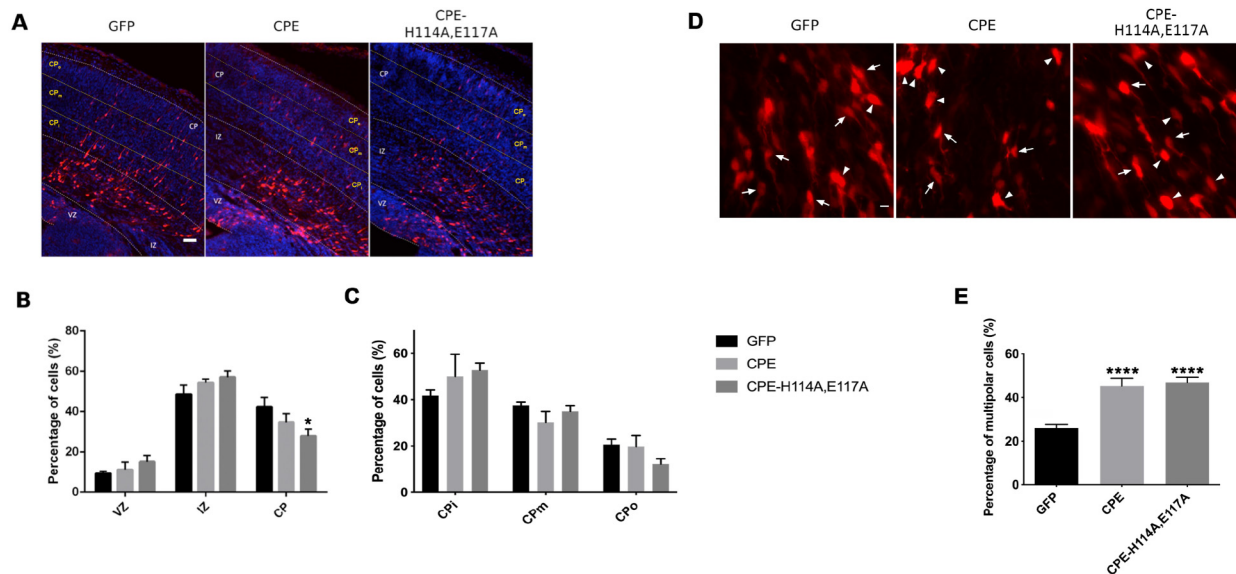


**Figure 5.** Overexpression of CPE-H114A,E117A alters overall cortical neuron migration. (A) Mice at E14.5 were co-electroporated *in utero* with pTagRFP and GFP (control) or carboxypeptidase E (CPE) constructs, and brains were analyzed at E17.5. Representative images of coronal brain sections are shown for each condition. Scale bar = 50  $\mu$ m. (B, C) Quantitation of the percentage of transfected cells in each cortical area. Error bars indicate  $\pm$  SEM. For (B): n = 8, GFP; n = 4, CPE; n = 5, CPE-H114A, E117A. For D: n = 14, GFP, n = 4, CPE, n = 4, CPE-H114A, E117A. \* $p < 0.05$  was determined by two-way ANOVA followed by Tukey's multiple comparisons test. Comparisons are to the GFP (control) group. (D) Representative images of transfected cells in the IZ of coronal brain sections after *in utero* electroporation with constructs as indicated that were analyzed for multipolar to bipolar transition. Arrows point to unipolar or bipolar cells; arrowheads point to multipolar cells. Scale bar = 20  $\mu$ m. (E) Quantitation of the percentage of multipolar transfected cells. Error bars indicate  $\pm$  SEM, n = 11, GFP; n = 4, CPE; n = 4, CPE-H114A, E117A. \*\* $p < 0.01$ , \*\*\* $p < 0.001$  was determined by two-way ANOVA followed by Dunnett's multiple comparisons test. Comparisons are to the GFP (control) group. Notes: Red = transfected cells; Blue = Hoechst dye. VZ = ventricular zone; IZ = intermediate zone; CP = cortical plate; CP<sub>i</sub> = inner cortical plate; CP<sub>m</sub> = middle cortical plate; CP<sub>o</sub> = outer cortical plate.

regulate substrate targeting or enzymatic activity. Indeed, immunoprecipitation of mouse brain polyglutamylase suggests that this enzyme may exist as a multimeric complex; a subunit of the complex, PGs1, regulates localization of the enzyme (Regnard et al., 2003). Furthermore, we specifically assessed the effects of CPE on polyglutamylated  $\alpha$ -tubulin. It is also possible that CPE affects polyglutamylation of  $\beta$ -tubulin.

### The Zinc-Binding Motif of CPE is Necessary but Sufficient to Promote CPE Action on p150<sup>Glued</sup> Localization

CPE expression begins early and increases dramatically during embryonic development (Birch et al., 1990), (Zheng et al., 1994). Roles for CPE in the endocrine and nervous systems as a prohormone-processing enzyme, sorting receptor, and mediator of vesicular transport have been reported by multiple groups (reviewed in Cawley et al., 2012). However, knowledge about how CPE contributes to neuronal development is only beginning to emerge (Loh et al., 2002). We reported previously that CPE and its interactor, p150<sup>Glued</sup> function to control cortical

development and dendrite morphogenesis (Liang et al., 2019), and others have reported a role for CPE in dendritic arborization and spine morphology *in vivo* (Woronowicz et al., 2010), neuronal degeneration and memory deficits (Woronowicz et al., 2008), dysfunction of BDNF signaling (Xiao et al., 2017), and neuronal protection from injury (Cheng et al., 2013; Cheng et al., 2015). CPE may regulate neuronal function, at least in part, by mediating effects on the MT network and MT-associated proteins (Liang et al., 2019).

CPE overexpression alters the localization of p150<sup>Glued</sup>, a protein that anchors MTs at the centrosome and binds to MT plus-ends (Liang et al., 2019; Askham, 2002; Berrueta et al., 1999; Quintyne et al., 1999), and this relocalization is dependent on the interaction between CPE carboxyl terminus and p150<sup>Glued</sup> (Liang et al., 2019). Since polyglutamylation influences protein binding to MTs, CPE may affect p150<sup>Glued</sup> localization by regulating levels of MT polyglutamylation, and thus, changes to p150<sup>Glued</sup> binding affinity to centrioles or MTs. Interestingly, we found that the zinc-binding motif and CPE-mediated changes to polyglutamylation are necessary, but not sufficient, for regulating p150<sup>Glued</sup> localization. Together with our previous findings, we provide new insights into CPE-mediated regulation of

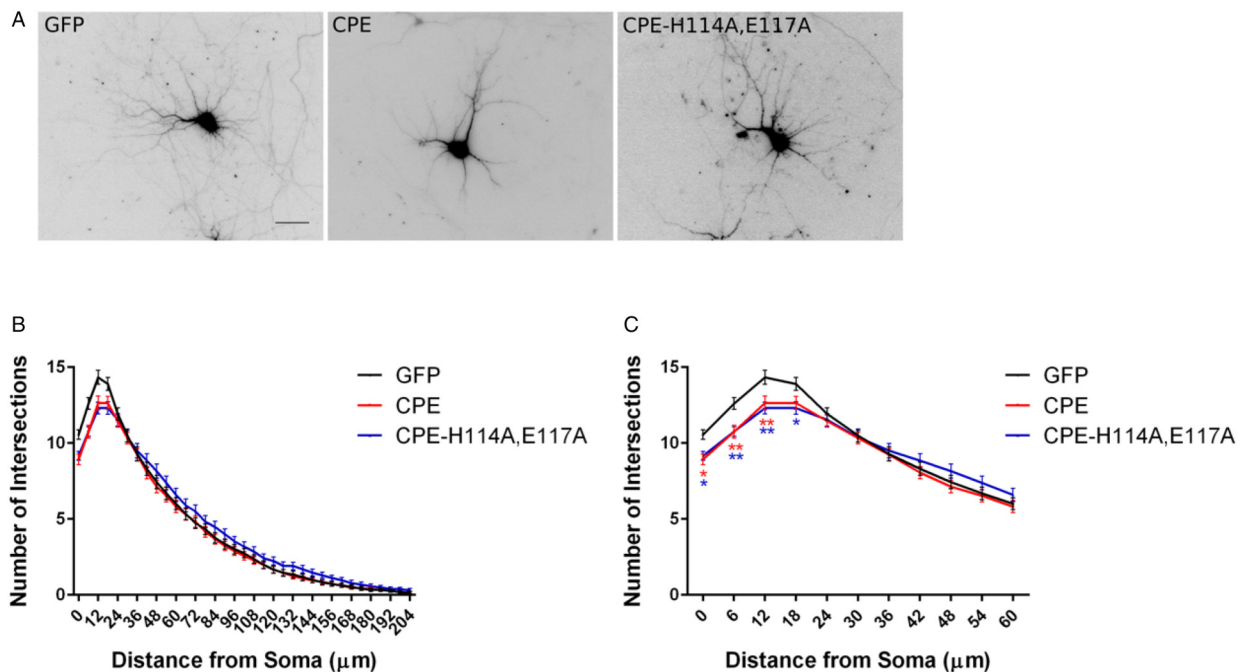


**Figure 6.** Overexpression of carboxypeptidase E (CPE) decreases proximal dendritic arborization in cultured hippocampal neurons and is not dependent on zinc-binding. (A) Rat hippocampal neurons were co-transfected with pCAG-mOrange (to visualize dendrites) and pEGFP (GFP), pEGFP-CPE (CPE), or pEGFP-CPE-H114A,E117A (CPE-H114A,E117A) at DIV 7. Neurons were fixed and immunostained for GFP and MAP2 at DIV 10. Neurons positive for both GFP and mOrange were used for Sholl analysis. Representative mOrange fluorescent images of neurons are shown as inverted black images. Scale bar = 50  $\mu\text{m}$ . (B) Sholl analysis of neurons overexpressing GFP, CPE, or CPE-H114A,E117A. (C) Sholl analysis from (B) within 60  $\mu\text{m}$  from the soma. Comparisons are to the GFP (control) group. Error bars indicate  $\pm$  SEM, n (neurons) = 95, GFP; n = 96, CPE; n = 93, CPE-H114A,E117A. \* $p < 0.05$ , \*\* $p < 0.01$  was determined by two-way ANOVA followed by Bonferroni multiple comparisons test.

p150<sup>Glued</sup> localization, suggesting the involvement of the CPE zinc-binding motif.

### *The Zinc-Binding Motif of CPE Plays a Role in Neuronal Migration but not in the Regulation of Dendrite Morphology*

Our previous work shows that CPE is required for proper cortical cell migration and dendrite branching (Liang et al., 2019). Knockdown of CPE protein *in utero* of E14.5 mice results in an increased percentage of cells found in the IZ at E17.5 and fewer cells located in the CP compared to control (Liang et al., 2019). In cultured neurons, both overexpression and knockdown of CPE protein lead to decreased dendrite branching, suggesting that a balance of CPE protein level is required for normal dendritogenesis (Liang et al., 2019).

MT polyglutamylation is controlled in a graded manner (Valenstein & Roll-Mecak, 2016), and disrupted polyglutamylation levels, and the requirement for MT glutamylation may be different for cortical neuron migration and changes to morphology. Resulting alterations in binding of MAPs and motor proteins to MTs from disrupted polyglutamylation may cause abnormalities in neuronal development.

The observation that CCP1, a deglutamylase also known as Nna1, is specifically expressed in differentiating neurons during brain development and upregulated in regenerating motor neurons after injury (Harris et al., 2000) also suggests a role for polyglutamylation in neurite outgrowth. Mutations in the glutamylase TTL5 that reduce glutamylation levels have been linked to retinal degeneration (Bedoni et al., 2016; Lee et al., 2013; Sergouniotis et al., 2014). Furthermore, mutations in the deglutamylase CCP1 that result in excess MT glutamylation contribute to neurodegeneration (Rogowski et al., 2010).

We observed that expression of CPE-H114A,E117A disrupts neuronal migration, indicating the necessity of the CPE zinc-binding motif in normal cortical development. Interestingly, CPE-H114A,E117A-mediated disruptions in neuronal migration are similar to those observed with shRNA-mediated knockdown of CPE, in which there was a decreased percentage of cells in the CP (Liang et al., 2019). Two possible explanations may exist for this result. First, CPE-mediated changes to tubulin polyglutamylation may not be involved in neuronal migration since overexpression of CPE does not show disrupted migration (Liang et al., 2019). The binding of zinc to CPE may regulate other functions of CPE. Alternatively, CPE-H114A,E117A may act in

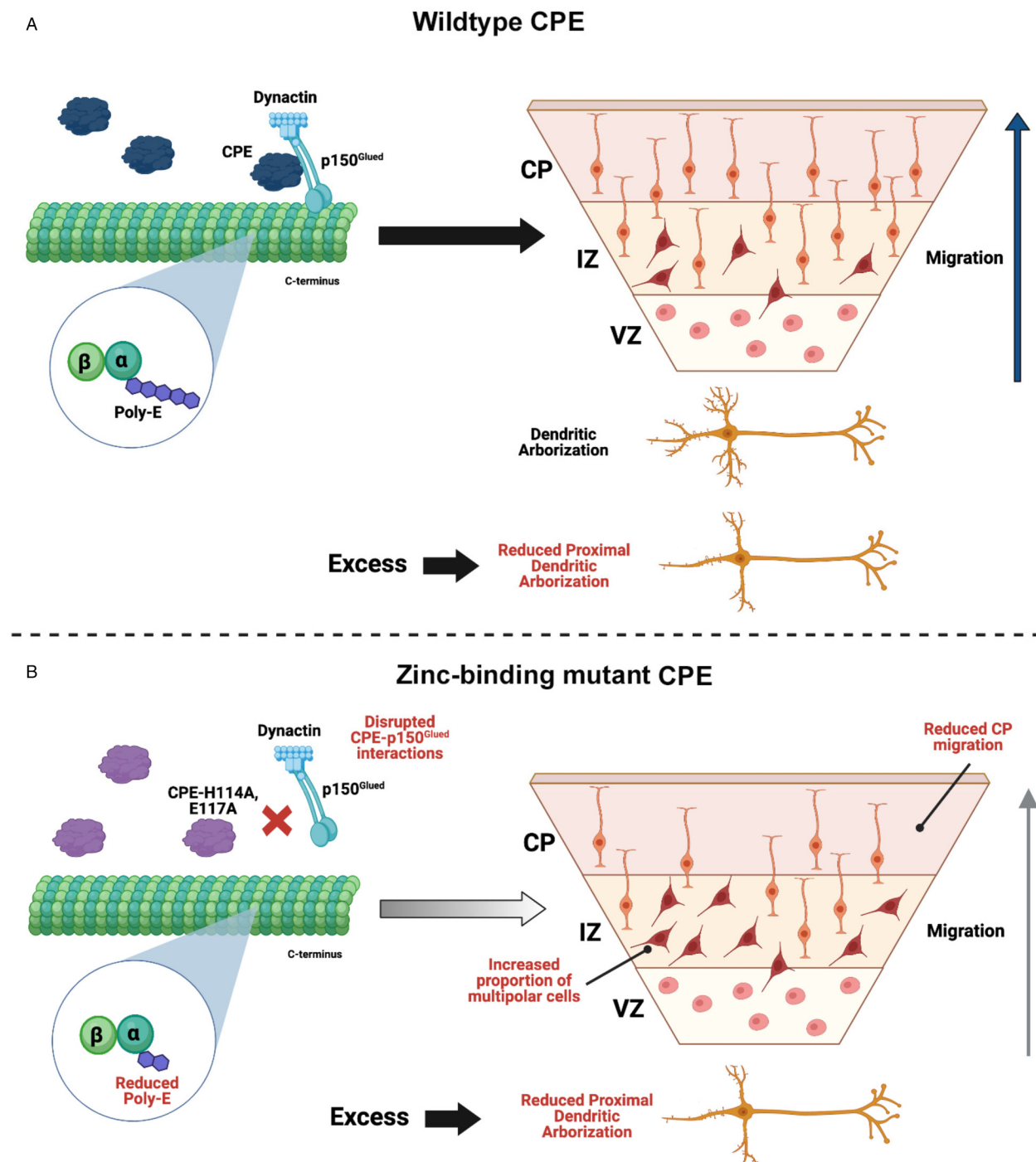


**Figure 7.** Model for the role of carboxypeptidase E (CPE)- mediated polyglutamylation in neuronal development. (A) CPE modulates microtubule (MT) dynamics, which ultimately facilitate proper neuronal migration and dendritic arborization during development. CPE binds to and prevents the localization of p150<sup>Glued</sup> to the centrosome through its C-terminal interacting motif. Free CPE and p150<sup>Glued</sup>-bound CPE further influence MT dynamics and stability by directly or indirectly catalyzing polyglutamylation of tubulin. However, maintenance of CPE expression and polyglutamylation levels within a critical threshold may be necessary for proper neuronal development. (B) Mutation of the zinc-binding motif prevents interaction between CPE and p150<sup>Glued</sup> and CPE-mediated changes to polyglutamylation, partially attenuates p150<sup>Glued</sup> localization at the centrosome, decreases neuronal migration to the CP, and increases the percentage of multipolar cells in the intermediate zone (IZ). As is the case with wild-type CPE, overexpression of mutant CPE decreases proximal dendritic arborization, suggesting a dose-dependent effect on dendrite morphology that is independent of CPE-mediated glutamylation. Created with BioRender.com.



a dominant-negative manner and disrupt normal function of endogenous CPE protein.

Surprisingly, in hippocampal neuronal cultures, overexpression of CPE-H114A,E117A results in the same phenotypes in dendrite architecture as does wild type CPE, suggesting that the zinc-binding motif is not involved in regulation of dendritogenesis. It is possible that the decrease in dendrite branching caused by CPE overexpression is not related to the increase in MT polyglutamylation at the time point we examined but is solely dependent on the interaction between the carboxyl terminus of CPE and p150<sup>Glued</sup>. However, we observed decreases in dendritic branching in cortical neurons *in vivo* and hippocampal neurons *in vitro* upon knockdown of CPE (Liang et al., 2019). It has been previously shown that both increased and decreased levels of tubulin polyglutamylation outside of a critical threshold can reduce the extent of spastin-mediated MT severing (Valenstein & Roll-Mecak, 2016), and MT dynamics contribute significantly to neuronal architecture (Penazzi et al., 2016). Thus, CPE-H114A,E117A acting in a dominant-negative manner as discussed above and recapitulating the effects of CPE knockdown on polyglutamylation to decrease dendritic arborization is also a possible mechanism of CPE action.

### Model for the Role of CPE-Mediated Polyglutamylation in Neuronal Development

Based on our findings, we propose the following model for the mechanism and effects of CPE-mediated polyglutamylation on dendritic arborization and neuronal migration during brain development (Figure 7). CPE binds to and prevents the localization of p150<sup>Glued</sup> (and possibly other MAPs) to the centrosome through its C-terminal interacting motif. Free CPE and p150<sup>Glued</sup>-bound CPE further influence MT dynamics and stability by directly or indirectly catalyzing polyglutamylation of tubulin, a PTM that modulates MT-associated protein interactions and MT severing. CPE-mediated changes to polyglutamylation are dependent on zinc binding, and interaction of CPE with p150<sup>Glued</sup> is partially dependent on the activity of the CPE zinc-binding motif. All of these functions of CPE contribute to the modulation of MT dynamics, which ultimately facilitate proper neuronal migration and dendritic arborization during development. However, maintenance of CPE expression and polyglutamylation levels within a critical threshold may be necessary to ensure proper neuronal development.

In summary, our study reports the identification of a novel function for CPE in promoting changes to tubulin polyglutamylation, and our data suggest that the zinc-binding motif is essential for mediating this effect. Moreover, we show that the CPE zinc-binding motif and CPE-mediated changes to polyglutamylation do not regulate dendrite morphogenesis but that the CPE zinc-binding motif is necessary for proper

cortical neuron migration. Taken together with our previous results (Liang et al., 2019), the zinc-binding and p150<sup>Glued</sup> interacting motifs of CPE play distinct roles in CPE function.

### Author's Contribution

Conceptualization, C.L. and B.L.F.; methodology, C.L., D.C., N.K.S., I.F., H.K., B.L.F.; formal analysis, C.L., D.C., N.K.S., L.L.H., and B.L.F.; investigation, C.L., D.C., N.K.S., I.F., and H.K.; data curation, C.L., D.C., N.K.S., and I.F.; writing—original draft preparation, C.L., D.C., N.K.S., L.L.H., and B.L.F.; writing—review and editing, C.L., D.C., N.K.S., L.L.H., and B.L.F.; project administration, B.L.F.; funding acquisition, B.L.F. All authors have read and agreed to the published version of the manuscript.

### Data Availability Statement

The data presented in this study are available upon request from the corresponding author.

### Declaration of Conflicting Interests

The author(s) declared no potential conflicts of interest with respect to the research, authorship, and/or publication of this article.

### Funding

The author(s) disclosed receipt of the following financial support for the research, authorship, and/or publication of this article: This work was supported by the National Science Foundation (grant number IOS-1353724), New Jersey Commission on Brain Injury Research (grant number CBIR17IRG006), National Institute of General Medical Sciences (grant number T32 GM008339-28), New Jersey Commission on Spinal Cord Research (grant number CSCR20FEL004), and an Aresty Research Center Fellowship.

### Institutional Review Board Statement

The study was conducted according to the guidelines of the Rutgers University Institutional Animal Care and Use Committee (Protocol PROTO999900080, most recent triennial approval February 2, 2020).

### ORCID iD

Bonnie L. Firestein  <https://orcid.org/0000-0002-1679-3565>

### References

- Akum, B. F., Chen, M., Gunderson, S. I., Riefler, G. M., Scerri-Hansen, M. M., Firestein, B. L. (2004). Cypin regulates dendrite patterning in hippocampal neurons by promoting microtubule assembly. *Nature Neuroscience*, 7(2), 145–152. doi: 10.1038/nm1179.
- Aloy, P., Companys, V., Vendrell, J., Aviles, F. X., Fricker, L. D., Coll, M., Gomis-Ruth, F. X. (2001). The crystal structure of the inhibitor-complexed carboxypeptidase D domain II and the modeling of regulatory carboxypeptidases. *Journal of Biological Chemistry*, 276(19), 16177–16184. doi: 10.1074/jbc.M011457200.
- Askham, J. M. (2002). Evidence that an interaction between EB1 and p150<sup>Glued</sup> is required for the formation and maintenance of a radial microtubule array anchored at the centrosome. *Molecular Biology of the Cell*, 13(10), 3627–3645. doi: 10.1091/mbc.e02-01-0061.

- Audebert, S., Desbruyeres, E., Gruszczynski, C., Koulakoff, A., Gros, F., Denoulet, P., Edde, B. (1993). Reversible polyglutamylation of alpha- and beta-tubulin and microtubule dynamics in mouse brain neurons. *Molecular Biology of the Cell*, 4(6), 615–626. doi: 10.1091/mbc.4.6.615.
- Audebert, S., Koulakoff, A., Berwald-Netter, Y., Gros, F., Denoulet, P., Edde, B. (1994). Developmental regulation of polyglutamylated alpha- and beta-tubulin in mouse brain neurons. *Journal of Cell Science*, 107(Pt 8), 2313–2322.
- Banker, G., Goslin, K. (1988). Developments in neuronal cell culture. *Nature*, 336(6195), 185–186. doi: 10.1038/336185a0.
- Bedoni, N., Haer-Wigman, L., Vaclavik, V., Tran, V. H., Farinelli, P., Balzano, S., Royer-Bertrand, B., El-Asrag, M. E., Bonny, O., Ikonomidis, C., Litzistorf, Y., Nikopoulos, K., Yioti, G. G., Stefanidou, M. I., McKibbin, M., Booth, A. P., Ellingford, J. M., Black, G.C., Toomes, C., ... Rivolta, C. (2016). Mutations in the polyglutamylase gene TLL5, expressed in photoreceptor cells and spermatozoa, are associated with cone-rod degeneration and reduced male fertility. *Human Molecular Genetics*, 25(20), 4546–4555. doi: 10.1093/hmg/ddw282.
- Berrueta, L., Tirnauer, J. S., Schuyler, S. C., Pellman, D., Bierer, B. E. (1999). The APC-associated protein EB1 associates with components of the dynactin complex and cytoplasmic dynein intermediate chain. *Current Biology*, 9(8), 425–428. doi: 10.1016/s0960-9822(99)80190-0.
- Birch, N. P., Rodriguez, C., Dixon, J.E., Mezey, E. (1990). Distribution of carboxypeptidase H messenger RNA in rat brain using in situ hybridization histochemistry: Implications for neuropeptide biosynthesis. *Molecular Brain Research*, 7(1), 53–59. doi: 10.1016/0169-328x(90)90073-m.
- Bonnet, C. (2001). Differential binding regulation of microtubule-associated proteins MAP1A, MAP1B, and MAP2 by tubulin polyglutamylase. *Journal of Biological Chemistry*, 276(16), 12839–12848. doi: 10.1074/jbc.M011380200.
- Boucher, D., Larcher, J. C., Gros, F., Denoulet, P. (1994). Polyglutamylase of tubulin as a progressive regulator of in vitro interactions between the microtubule-associated protein Tau and tubulin. *Biochemistry*, 33(41), 12471–12477. doi: 10.1021/bi00207a014.
- Carrel, D., Hernandez, K., Kwon, M., Mau, C., Trivedi, M. P., Brzustowicz, L. M., Firestein, B. L. (2015). Nitric oxide synthase 1 adaptor protein, a protein implicated in schizophrenia, controls radial migration of cortical neurons. *Biological Psychiatry*, 77(11), 969–978. doi: 10.1016/j.biopsych.2014.10.016.
- Cawley, N. X., Wetsel, W. C., Murthy, S. R. K., Park, J. J., Pacak, K., Loh, Y. P. (2012). New roles of carboxypeptidase E in endocrine and neural function and cancer. *Endocrine Reviews*, 33(2), 216–253. doi: 10.1210/er.2011-1039.
- Charych, E. I., Akum, B. F., Goldberg, J. S., Jörnsten, R. J., Rongo, C., Zheng, J. Q., Firestein, B. L. (2006). Activity-Independent regulation of dendrite patterning by postsynaptic density protein PSD-95. *Journal of Neuroscience*, 26(40), 10164–10176. doi: 10.1523/JNEUROSCI.2379-06.2006.
- Chen, H., Firestein, B. L. (2007). RhoA regulates dendrite branching in hippocampal neurons by decreasing cypin protein levels. *Journal of Neuroscience*, 27(31), 8378–8386. doi: 10.1523/JNEUROSCI.0872-07.2007.
- Cheng, Y., Cawley, N. X., Loh, Y. P. (2013). Carboxypeptidase E/NF $\alpha$ 1: A New neurotrophic factor against oxidative stress-induced apoptotic cell death mediated by ERK and PI3-K/AKT pathways. *PLoS ONE*, 8(8), e71578. doi: 10.1371/journal.pone.0071578.
- Cheng, Y., Cawley, N. X., Yanik, T., Murthy, S. R. K., Liu, C., Kasikci, F., Abebe, D., Loh, Y. P. (2016). A human carboxypeptidase E/NF- $\alpha$ 1 gene mutation in an Alzheimer's Disease patient leads to dementia and depression in mice. *Translational Psychiatry*, 6(12), e973–e973. doi: 10.1038/tp.2016.237.
- Cheng, Y., Rodriguiz, R. M., Murthy, S. R. K., Senatorov, V., Thouennon, E., Cawley, N. X., Aryal, D. K., Ahn, S., Lecka-Czernik, B., Wetsel, W. C., Loh, Y. P. (2015). Neurotrophic factor- $\alpha$ 1 prevents stress-induced depression through enhancement of neurogenesis and is activated by rosiglitazone. *Molecular Psychiatry*, 20(6), 744–754. doi: 10.1038/mp.2014.136.
- Dhanvantari, S., Shen, F.-S., Adams, T., Snell, C. R., Zhang, C., Mackin, R. B., Morris, S. J., Loh, Y. P. (2003). Disruption of a receptor-mediated mechanism for intracellular sorting of proinsulin in familial hyperproinsulinemia. *Molecular Endocrinology*, 17(9), 1856–1867. doi: 10.1210/me.2002-0380.
- Dotti, C., Sullivan, C., Banker, G. (1988). The establishment of polarity by hippocampal neurons in culture. *Journal of Neuroscience*, 8(4), 1454–1468. doi: 10.1523/JNEUROSCI.08-04-01454.1988.
- Fricker, L. D., Snyder, S. H. (1982). Enkephalin convertase: Purification and characterization of a specific enkephalin-synthesizing carboxypeptidase localized to adrenal chromaffin granules. *Proceedings of the National Academy of Sciences*, 79(12), 3886–3890. doi: 10.1073/pnas.79.12.3886.
- Gomis-Ruth, F. X., Companys, V., Qian, Y., Fricker, L. D., Vendrell, J., Avilés, F. X., Coll, M. (1999). Crystal structure of avian carboxypeptidase D domain II: A prototype for the regulatory metallo-carboxypeptidase subfamily. *The EMBO Journal*, 18(21), 5817–5826. doi: 10.1093/emboj/18.21.5817.
- Harris, A., Morgan, J. I., Pecot, M., Soumare, A., Osborne, A., Soares, H. D. (2000). Regenerating motor neurons express Nna1, a novel ATP/GTP-binding protein related to zinc carboxypeptidases. *Molecular and Cellular Neuroscience*, 16(5), 578–596. doi: 10.1006/mcne.2000.0900.
- Hook, V. Y. H., Eiden, L. E., Brownstein, M. J. (1982). A carboxypeptidase processing enzyme for enkephalin precursors. *Nature*, 295(5847), 341–342. doi: 10.1038/295341a0.
- Hutton, J. C., Davidson, H. W., Peshavaria, M. (1987). Proteolytic processing of chromogranin A in purified insulin granules. Formation of a 20 kDa N-terminal fragment (betagranin) by the concerted action of a Ca<sup>2+</sup>-dependent endopeptidase and carboxypeptidase H (EC 3.4.17.10). *Biochemical Journal*, 244(2), 457–464. doi: 10.1042/bj2440457.
- Ikegami, K., Mukai, M., Tsuchida, J.-I., Heier, R. L., Macgregor, G. R., Setou, M. (2006). TLL7 Is a mammalian  $\beta$ -tubulin polyglutamylase required for growth of MAP2-positive neurites. *Journal of Biological Chemistry*, 281(41), 30707–30716. doi: 10.1074/jbc.M603984200.
- Janke, C., Rogowski, K., Wloga, D., Regnard, C., Kajava, A. V., Strub, J.-M., Temurak, N., van Dijk, J., Boucher, D., van Dorsselaer, A., Suryavanshi, S., Gaertig, J., Eddé, B. (2005). Tubulin polyglutamylase enzymes Are members of the TTL domain protein family. *Science (New York, N Y)*, 308(5729), 1758–1762. doi: 10.1126/science.1113010.
- Kalinina, E., Biswas, R., Berezniuk, I., Hermoso, A., Aviles, F. X., Fricker, L. D. (2007). A novel subfamily of mouse cytosolic



- carboxypeptidases. *The FASEB Journal*, 21(3), 836–850. doi: 10.1096/fj.06-7329com.
- Kutzing, M. K., Langhammer, C. G., Luo, V., Lakdawala, H., Firestein, B. L. (2010). Automated sholl analysis of digitized neuronal morphology at multiple scales. *Journal of Visualized Experiments*, 45, 2354–2354. doi: 10.3791/2354.
- Langhammer, C. G., Previtera, M. L., Sweet, E. S., Sran, S. S., Chen, M., Firestein, B. L. (2010). Automated sholl analysis of digitized neuronal morphology at multiple scales: Whole cell sholl analysis versus sholl analysis of arbor subregions. *Cytometry Part A*, 77A(12), 1160–1168. doi: 10.1002/cyto.a.20954.
- Larcher, J.-C., Boucher, D., Lazereg, S., Gros, F., Denoulet, P. (1996). Interaction of kinesin motor domains with  $\alpha$ - and  $\beta$ -tubulin subunits at a Tau-independent binding site. *Journal of Biological Chemistry*, 271(36), 22117–22124. doi: 10.1074/jbc.271.36.22117.
- Lee, G. S., He, Y., Dougherty, E. J., Jimenez-Movilla, M., Avella, M., Grullon, S., Sharlin, D. S., Guo, C., Blackford Jr, J. R., Awasthi, S., Zhang, Z., Armstrong, S. P., London, E. C., Chen, W., Dean, J., Simons Jr, S. S. (2013). Disruption of Tll5/stamp gene (tubulin tyrosine ligase-like protein 5/SRC-1 and TIF2-associated modulatory protein gene) in male mice causes sperm malformation and infertility. *Journal of Biological Chemistry*, 288(21), 15167–15180. doi: 10.1074/jbc.M113.453936.
- Liang, C., Carrel, D., Omelchenko, A., Kim, H., Patel, A., Fanget, I., Firestein, B.L. (2019). Cortical neuron migration and dendrite morphology are regulated by carboxypeptidase E. *Cerebral Cortex*, 29(7), 2890–28903. doi: 10.1093/cercor/bhy155.
- Loh, Y. P., Maldonado, A., Zhang, C., Tam, W. H., Cawley, N. (2002). Mechanism of sorting proopiomelanocortin and proenkephalin to the regulated secretory pathway of neuroendocrine cells. *Annals of the New York Academy of Sciences*, 971(1), 416–425. doi: 10.1111/j.1749-6632.2002.tb04504.x.
- Lou, H., Kim, S.-K., Zaitsev, E., Snell, C. R., Lu, B., Loh, Y. P. (2005). Sorting and activity-dependent secretion of BDNF require interaction of a specific motif with the sorting receptor carboxypeptidase E. *Neuron*, 45(2), 245–255. doi: 10.1016/j.neuron.2004.12.037.
- Penazzi, L., Bakota, L., Brandt, R. (2016). Microtubule dynamics in neuronal development, plasticity, and neurodegeneration. *International Review of Cell and Molecular Biology*, 321, 89–169. doi: 10.1016/bs.ircmb.2015.09.004.
- Quintyne, N. J., Gill, S. R., Eckley, D. M., Crego, C. L., Compton, D. A., Schroer, T. A. (1999). Dynactin Is required for microtubule anchoring at centrosomes. *Journal of Cell Biology*, 147(2), 321–334. doi: 10.1083/jcb.147.2.321.
- Ramadan, Y. H., Gu, A., Ross, N., McEwan, S. A., Barr, M. M., Firestein, B. L., O'Hagan, R. (2021). CCP1, A tubulin deglutamyase, increases survival of rodent spinal cord neurons following glutamate-induced excitotoxicity. *Eneuro*, 8(2), 0431. doi: 10.1523/ENEURO.0431-20.2021.
- Regnard, C., Fesquet, D., Janke, C., Boucher, D., Desbruyères, E., Koulakoff, A., Insina, C., Travo, P., Eddé, B. (2003). Characterisation of PGs1, a subunit of a protein complex co-purifying with tubulin polyglutamylase. *Journal of Cell Science*, 116(20), 4181–4190. doi: 10.1242/jcs.00743.
- Reznik, S. E., Fricker, L. D. (2001). Carboxypeptidases from A to Z: Implications in embryonic development and Wnt binding. *Cellular and Molecular Life Sciences*, 58(12), 1790–1804. doi: 10.1007/PL00000819.
- Rodriguez de la Vega, M., Sevilla, R. G., Hermoso, A., Lorenzo, J., Tanco, S., Diez, A., Fricker, L. D., Bautista, J. M., Avilés, F. X. (2007). Nnal-like proteins are active metallo-carboxypeptidases of a new and diverse M14 subfamily. *The FASEB Journal*, 21(3), 851–865. doi: 10.1096/fj.06-7330com.
- Rogowski, K., van Dijk, J., Magiera, M. M., Bosc, C., Deloulme, J.-C., Bosson, A., Peris, L., Gold, N. D., Lacroix, B., Grau, M. B., Bec, N., Larroque, C., Desagher, S., Holzer, M., Andrieux, A., Moutin, M.-J., Janke, C. (2010). A family of protein-deglutamylating enzymes associated with neurodegeneration. *Cell*, 143(4), 564–578. doi: 10.1016/j.cell.2010.10.014.
- Sergouniotis, P. I., Chakarova, C., Murphy, C., Becker, M., Lenassi, E., Arno, G., Lek, M., MacArthur, D. G., UCL-Exomes Consortium, Bhattacharya, S. S., Moore, A. T., Holder, G. E., Robson, A. G., Wolfrum, U., Webster, A. R., Plagnol, V. (2014). Biallelic variants in TTLL5, encoding a tubulin glutamylase, cause retinal dystrophy. *The American Journal of Human Genetics*, 94(5), 760–769. doi: 10.1016/j.ajhg.2014.04.003.
- Tabata, H., Nagata, K. (2016). Decoding the molecular mechanisms of neuronal migration using in utero electroporation. *Medical Molecular Morphology*, 49(2), 63–75. doi: 10.1007/s00795-015-0127-y.
- Valenstein, M. L., Roll-Mecak, A. (2016). Graded control of microtubule severing by tubulin glutamylation. *Cell*, 164(5), 911–921. doi: 10.1016/j.cell.2016.01.019.
- van Dijk, J., Rogowski, K., Miro, J., Lacroix, B., Eddé, B., Janke, C. (2007). A targeted multienzyme mechanism for selective microtubule polyglutamylation. *Molecular Cell*, 26(3), 437–448. doi: 10.1016/j.molcel.2007.04.012.
- Woronowicz, A., Cawley, N. X., Chang, S.-Y., Koshimizu, H., Phillips, A. W., Xiong, Z.-G., Loh, Y. P. (2010). Carboxypeptidase E knockout mice exhibit abnormal dendritic arborization and spine morphology in central nervous system neurons. *Journal of Neuroscience Research*, 88(1), 64–72. doi: 10.1002/jnr.22174.
- Woronowicz, A., Koshimizu, H., Chang, S.-Y., Cawley, N. X., Hill, J. M., Rodriguez, R. M., Abebe, D., Dorfman, C., Senatorov, V., Zhou, A., Xiong, Z.-G., Wetsel, W. C., Loh, W. P. (2008). Absence of carboxypeptidase E leads to adult hippocampal neuronal degeneration and memory deficits. *Hippocampus*, 18(10), 1051–1063. doi: 10.1002/hipo.20462.
- Wu, H. Y., Wang, T., Li, L., Correia, K., Morgan, J. I. (2012). A structural and functional analysis of Nnal in purkinje cell degeneration (pcd) mice. *FASEB*, 26(11), 4468–4480.
- Xiao, L., Chang, S.-Y., Xiong, Z.-G., Selveraj, P., Loh, Y. P. (2017). Absence of carboxypeptidase E/neurotrophic factor-A1 in knock-Out mice leads to dysfunction of BDNF-TRKB signaling in hippocampus. *Journal of Molecular Neuroscience*, 62, 79–87. doi: 10.1007/s12031-017-0914-0.
- Xiao, L., Sharma, V. K., Toulabi, L., Yang, X., Lee, C., Abebe, D., Peltekian, A., Arnaoutova, I., Lou, H., Loh, Y. P. (2021). Neurotrophic factor- $\alpha$ 1, a novel tropin is critical for the prevention of stress-induced hippocampal CA3 cell death and cognitive dysfunction in mice: Comparison to BDNF. *Translational Psychiatry*, 11(1), 24–24. doi: 10.1038/s41398-020-01112-w.
- Zheng, M., Streck, R. D., Scott, R. E., Seidah, N. G., Pintar, J. E. (1994). The developmental expression in rat of proteases furin, PC1, PC2, and carboxypeptidase E: Implications for early maturation of proteolytic processing capacity. *Journal of Neuroscience*, 14(8), 4656–4673. doi: 10.1523/JNEUROSCI.14-08-04656.1994.